Selected Papers

Growth and Architecture of Single-Walled Carbon Nanotubes on Patterned Silicon Substrates

Yoshikazu Homma[†], Yoshihiro Kobayashi, and Toshio Ogino

Abstract

Single-walled carbon nanotubes (SWNTs) were grown on Si and SiO₂ patterns to form self-assembled interconnecting networks. The growth was performed by chemical vapor deposition using methane and Fe catalyst. Arrays of Si or SiO_2 nano-pillars were prepared using synchrotron-radiation lithography. The SWNT yield was controlled by choosing the catalyst particle size and growth temperature. When the SWNT yield was low, a suspended network of individual SWNTs formed. The bridging SWNTs were fairly straight, but the network density was low. At higher yields, bundles of SWNTs formed, and almost all the pillars were connected in the SWNT bundle network. Suspended SWNTs will be useful for wiring or for the site-selective formation of SWNT-based transistors. They also show enhanced Raman and photoluminescence signals. Thus, suspended SWNTs are of interest for both electronic and optical applications.

1. Introduction

Carbon nanotubes, nano-scale cylinders of carbon, have remarkable mechanical, electrical, and chemical properties and are expected to be used for various applications in nanoelectronics [1]. They are self-organizing and can be semiconducting or metallic. Semiconducting carbon nanotubes act as field effect transistors [2] or single electron transistors [3], and they have shown single electron transistor characteristics even at room temperature [4]. Metallic carbon nanotubes, on the other hand, exhibit ballistic conductivity at room temperature [5], and this along with their mechanical strength, shape, and size makes them ideal for the wiring of nano-scale devices. However, before we can build nanotube-based integrated circuits, we must be able to control the chirality of nanotubes[*1] as well as their growth site, growth direction, and length. To control the growth site and direction, Cassell et al. used arrays of 10-μm-high silicon towers and grew a network of nanotubes connecting the towers by chemical vapor deposition (CVD) [6], [7]. This self-directed growth is a remarkable feature of carbon nanotubes. However, the growth mechanism is not understood yet. We are attempting to use the self-directed growth of nanotubes on patterned substrates to fabricate nanotube interconnections between nanostructures. In this paper, we report the synthesis of single-walled carbon nanotube (SWNT) networks on an array of sub-micrometer-scale Si or SiO_2 pillars. Carbon nanotubes were grown using CVD with Fe catalysts. We succeeded in fabricating various nanotube architectures. We found that SWNTs suspended on the pillars showed enhanced Raman and photoluminescence signals, which is useful in applications to nanotube devices as well as nanotube characterization. The self-directed growth mechanism is also discussed based on our observations using scanning electron microscopy.

† NTT Basic Research Laboratories
  Atsugi-shi, 243-0198 Japan
  E-mail: homma@will.brl.ntt.co.jp

*1 The chirality of nanotubes lets us characterize the arrangement of atoms in the nanotube, and determine how a graphite layer is rolled into a cylindrical shape.

2. Selective growth of SWNTs on silicon substrates

Carbon nanotubes were grown by CVD using methane as the carbon source and Fe as the catalyst. For the catalyst preparation, a thin film of Fe was deposited on a Si or SiO_2 substrate using a conventional vacuum evaporator. The thickness of the deposited film varied from 0.2 to 5 nm. The deposited film turned into particles during thermal treatment in CVD growth, and the particle size depended on the film thickness. The Fe particle sizes were 5 and 50 nm for 0.5- and 5-nm films, respectively. The furnace for CVD experiments is described elsewhere [8]. An argon gas flowed as the furnace was heated to reach growth temperature (700–950°C). The argon gas was then replaced by pure methane at a flow rate of 300 cm^3/min with the pressure of 67 kPa. The methane flowed for 1 min and then was replaced by argon to cool the furnace to room temperature. After growth,

the specimens were observed with a high-resolution scanning electron microscope (SEM) and a transmission electron microscope (TEM).

In methane CVD with Fe catalyst, the nanotube species grown depends on the growth temperature and the Fe catalyst particle size. When the particle size is 10-30 nm, SWNTs grow at 950–900°C, and multi-walled nanotubes (MWNTs) grow at around 800°C [8]. The SWNT growth temperature is lower for smaller Fe particles. SWNTs can be obtained at 750°C or higher for 5-nm particles. The density of SWNTs is higher for smaller Fe particles. **Figure 1** shows SEM images of SWNTs grown on Si and SiO_2 substrates. When the Fe film thickness was around 1 nm, most of the nanotubes were individual SWNTs (**Figs. 1(a)** and **1(c)**), though there was a slight difference in the temperature range between Si and SiO_2 substrates. For smaller Fe particles, SWNTs formed bundles (**Figs. 1(b)** and **1(d)**). Since the SWNT yield was higher for the SiO_2 substrates, the bundles were
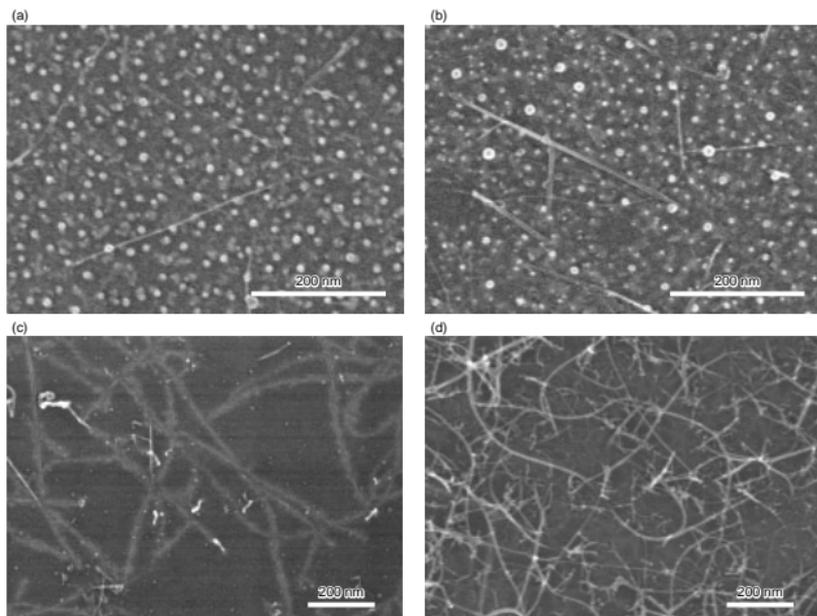

Fig. 1. SEM images of SWNTs on Si and SiO_2 substrates grown at 900°C using Fe catalyst films with different thickness. (a) 1-nm Fe film on Si, (b) 0.5-nm Fe film on Si, (c) 0.5-nm Fe film on SiO_2, and (d) 0.2-nm Fe film on SiO_2.

much denser on them. The reason for the differences between Si and SiO$_2$ substrates lies in how the Fe catalyst reacts with each substrate.

On Si substrate, SiO$_2$ surrounds the Fe particles after annealing of the substrate in argon. **Figure 2(a)** shows an SEM image of a Si substrate surface after CVD growth. The particles are surrounded by a substance of weaker contrast, which is SiO$_2$ [8]. Similar images can be seen in Figs. 1(a) and (b). The free-energy difference between SiO$_2$ and Fe$_2$O$_3$ might contribute to the favorable reduction of oxide around the Fe particles, so SiO$_2$ is formed selectively around them. The SiO$_2$ base is thought to prevent the reaction between Fe particles and Si substrate. When the substrate temperature is high, a reaction occurs between the catalyst and the Si substrate. At silicide formation temperatures, nanotubes are rarely formed [9]. However, Fe particles are not always fully isolated from the Si substrate by SiO$_2$. When they partially touch the substrate, silicidation can occur (**Figs. 2(b)** and **2(c)**). This might be the reason for the lower SWNT yield on Si compared to that on SiO$_2$. On the SiO$_2$ surface, Fe particles do not form silicide below 1000°C, but they are often embedded under the surface (**Fig. 2(d)**). Even so, the SWNT yield is rather high on the SiO$_2$ surface. This is a curious phenomenon and should be investigated further.

3. Suspended SWNT network growth on patterned substrates

By using the selectivity in growing individual SWNTs or bundles of SWNTs, we could obtain various SWNT architectures on patterned substrates. Arrays of Si or SiO$_2$ pillars were prepared using synchrotron-radiation lithography. The pillar patterns consisted of a two-dimensional square lattice of cylindrical pillars (diameter: 150 nm, height: 360 nm for Si and 300 nm for SiO$_2$, pitch: 400–1000 nm). SWNTs grown on pillar structures frequently showed suspended growth between pillars. **Figure 3** shows SEM images of individual SWNTs and bundles of SWNTs suspended from the SiO$_2$ pillars. When the SWNT yield was low, the suspended nanotubes consisted of individual SWNTs. The SWNTs were fairly straight, but the density was low. Some pillars had no suspended nanotubes (**Fig. 3(a)**). At higher yields, SWNT bundles were formed (**Fig. 3(b)**). Interestingly, nanotubes from each pillar bundled together to make a single bridge between neighboring pillars.

Figure 4(a) shows individual SWNTs grown on 100-nm-diameter Si pillars [10]. Most of the SWNTs
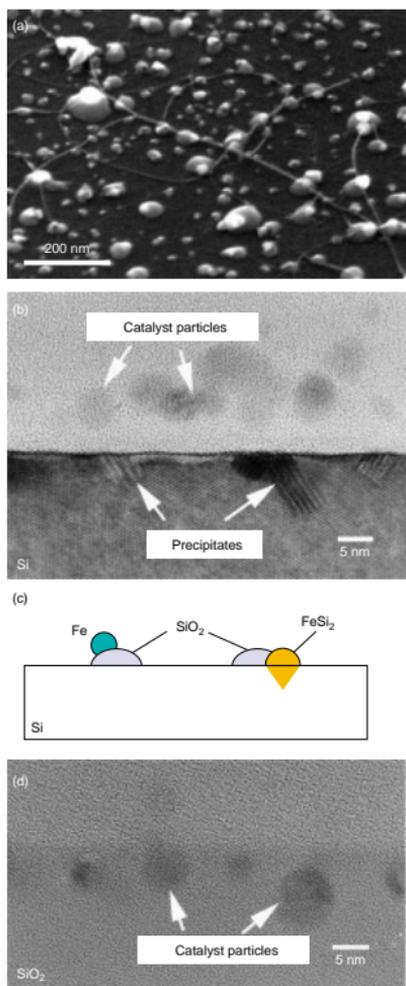

Fig. 2. SEM and TEM images of Fe particles on Si and SiO$_2$ substrates after CVD. (a) SEM image of Fe particles on Si, (b) cross-sectional TEM image of Fe particles on Si, (c) schematic illustration of Fe particles on Si, and (d) cross-sectional TEM image of Fe particles on SiO$_2$.
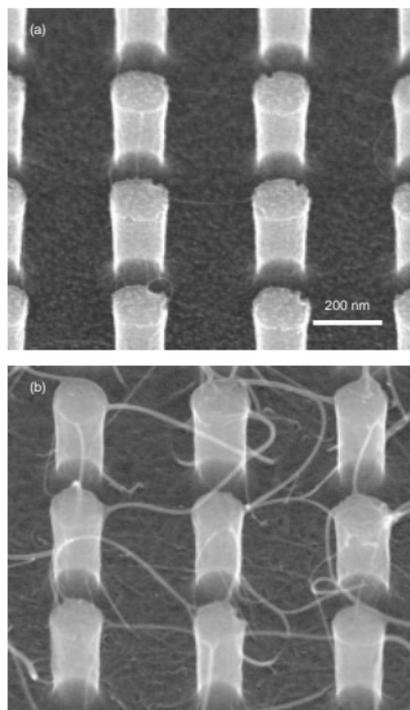
Fig. 3. SEM images of SWNT bridges on SiO$_2$ pillars. (a) Individual SWNT bridges and (b) bridges consisting of SWNT bundles.

started growing from the pillar tops and reached adjacent pillars, forming a network structure. Some nanotubes extended from one pillar to another, and others just reached a neighboring pillar and stopped. Most reached the nearest neighbor, but some connected to the second-nearest neighbors.

Figures 4(b) and **4(c)** show the bundle growth on Si and SiO$_2$ pillars, respectively. The catalyst film was deposited after tilting the substrate +45° and then −45° [11]. Thus, the catalyst film formed on the sidewalls as well as on the tops of pillars. Nevertheless, the bundles were suspended only between the tops of the Si pillars (Fig. 4(b)). This means that the SWNTs that grew on the sidewalls of the pillars might have bundled together at the pillar top. The number of

bridges suspended between neighboring pillars was roughly one. The bundles were often curved, but almost all the pillars were connected in the SWNT bundle network. Bundles also formed bridges between the SiO$_2$ pillars, but many individual bundles extended from sidewall to sidewall (Fig. 4(c)). That is, the pillars were connected by many bundles, which is in sharp contrast to the Si pillar case. The SWNT yield difference between Si and SiO$_2$ is the reason for the marked change of the suspended structures.

4. Properties of suspended SWNTs

The difference between the suspended SWNTs and the SWNTs on the substrate is that the suspended ones do not interact with the substrate. This is a simple and obvious difference, but it has a significant effect on SWNT properties. In this respect, individual suspended SWNTs are the most interesting because they are also free from interaction with other nanotubes.

We have found some remarkable properties specific to suspended SWNTs. One is the observation of intense Raman signals from suspended SWNTs [12]. SWNTs show various Raman modes, by which the structures of individual nanotubes can be characterized. The Raman signals from suspended SWNTs are much more intense than those from SWNTs on the substrate. **Figure 5** shows Raman signals obtained by scanning the probe laser beam from the flat region to the pillar region. In the measured wave number range, there is a G-band ($\approx$1590 cm^{-1}) originating from the in-plane stretching mode of the graphite sheet and a D-band ($\approx$1530 cm^{-1}) originating from defects. The number of SWNTs on the substrate surface was more than 100 times that of suspended SWNTs. Nevertheless, the intensity of the G- and D- bands was stronger in the pillar region. This indicates that even one SWNT can be detected by Raman spectroscopy when it is suspended.

Another interesting and very important result is that the suspended SWNTs are photoluminescent. Semiconducting SWNTs have a direct-band-gap structure, and thus should be luminescent for the band-gap transition. However, so far, SWNT bundles or SWNTs on the substrate have not shown luminescence; only solutions of purified SWNTs individually isolated inside surfactant micelles were reported to be luminescent [13]. We recently found that the suspended SWNTs show intense band-gap luminescence in the near-infrared region [14], [15]. The precise mechanism has not been clarified yet, but isolating the
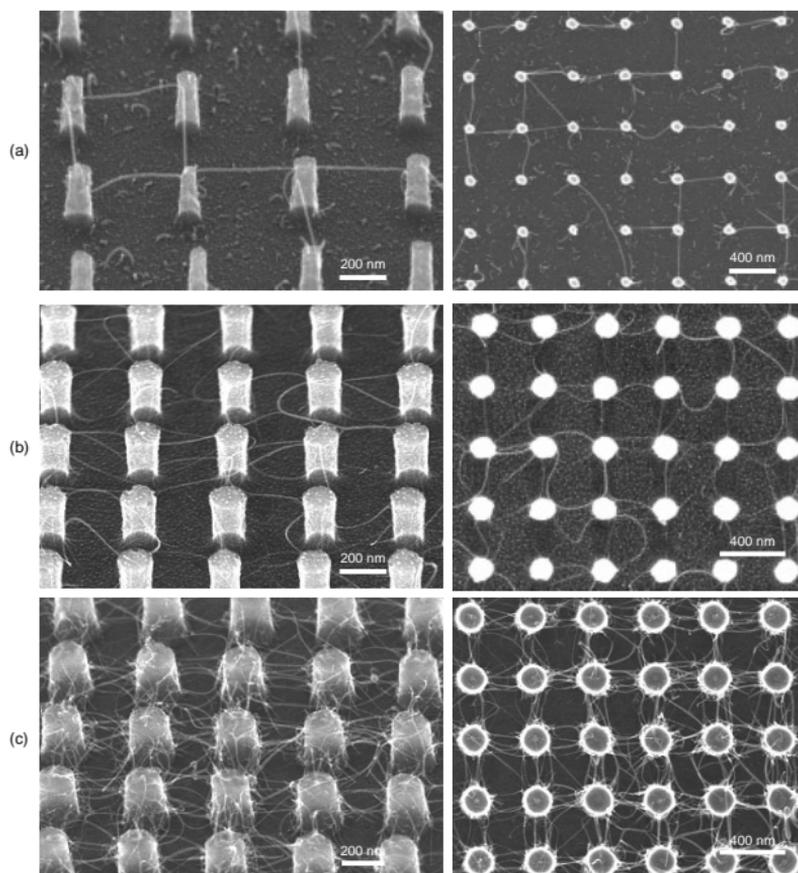
Fig. 4.   SEM images of various SWNT architectures at glancing and top views. (a) Individual SWNT bridges (Pt-coated) on Si pillars, (b) bundle SWNT bridges on Si pillars, and (c) multiple bridges of SWNT bundles on SiO₂ pillars.

SWNTs by minimizing their interaction with the environment is the key to obtaining luminescence. This is a very important finding because it means that suspended SWNTs may be able to emit light at optical communication wavelengths of 1.3 or 1.55 µm. The excitation and emission wavelengths depend on the chirality of SWNTs. Therefore, controlling the chirality is a crucial issue for future applications.

5.   Mechanism of suspended growth

The growth of nanotubes suspended between the pillars was investigated statistically through SEM observations of about 2000 pillars [10]. The results for a mostly individual SWNT case are summarized in **Fig. 6**. About 76% of the pillars examined showed nanotube growth in some style. Among them, 45%

were bridging nanotubes, 40% fallen ones, and 15% halfway terminated ones. Among the bridging nanotubes, 85% achieved nearest-neighbor connection,
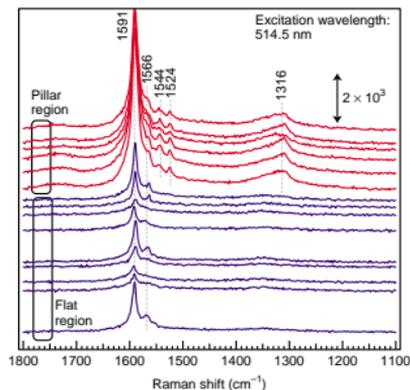

Fig. 5. Comparison of Raman spectra between the pillar region and flat region.

while only 9% showed second-nearest neighbor connection. Therefore, 29% of the nanotubes originating from the pillar top achieved interconnection between nearest-neighbor pillars.

Such a relatively large fraction of the nearest-neighbor interconnection can be obtained when the pillar aspect ratio is large and the pillar spacing is less than twice the pillar height. When the pattern spacing was much larger than the pillar height, nanotubes often failed to connect to pillars directly and fell to the substrate. However, the difference in the spacing between the nearest neighbor and the second-nearest neighbor cannot explain the large difference in yield, because when the pillar spacing was less than twice the pillar height, the percentages of nearest- and second-nearest-neighbor bridging were almost constant. The methane flow, which is supposed to keep the nanotubes floating [7], is unlikely to be the cause of the suspended growth because of the lower pressure and smaller methane flow rate in the present case. In addition, we did not observe any flow direction effects.

Nanotubes originating from pillar tops can extend in any direction. However, if a nanotube starts to grow on the plane of the pillar top, the tube is likely to grow along the pillar top surface and thus extend
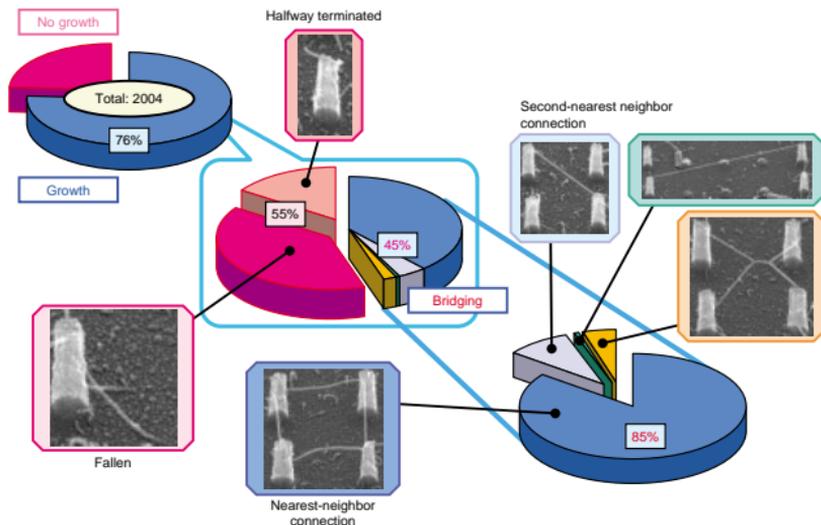

Fig. 6. Percentages of nanotube types grown on Si pillars using Fe catalyst.

parallel to the substrate surface. As a nanotube extends, it forms a cantilever with a large aspect ratio, so the open end of the nanotube vibrates during extension. If the vibration amplitude is large, the nanotube contacts a neighboring pillar. The thermal vibration amplitude of a SWNT at 900°C was estimated to be as large as 6 μm when the tube length L was 20 μm [16]. However, the amplitude is proportional to $L^{3/2}$ [17], and it is estimated to be only 18 nm for a 400-nm-long SWNT. This value is quite modest and cannot explain the high percentage of nearest-neighbor bridging. Furthermore, the vibration frequency of a SWNT calculated using the equation in Ref. 17 is of the order of 10^8 MHz, which could hardly include any enhancement from the mechanical vibration of the CVD apparatus. One explanation for this discrepancy is imperfections in the CVD-grown nanotubes. The above values assume a Young's modulus of 1 TPa. However, because of the lower growth temperature in CVD, the nanotubes are defective compared with those grown by laser ablation or arc discharge. In addition, when bundles are formed, the effective Young's modulus decreases with increasing bundle diameter [18]. If the effective Young's modulus decreases by a factor of 100, the thermal vibration amplitude becomes 180 nm for a 400-nm cantilever. This explanation can be applied to the bundle case, where the bridges curve substantially, showing a reduced effective Young's modulus. However, for individual SWNTs, a decrease in Young's modulus by a factor of 100 cannot be attributed only to defects.

We have shown that the catalyst particles melt in the growth ambient [9]. Therefore, when a nanotube contacts a pillar only at a catalyst particle, the nanotube may swing or even revolve around the particle due to the mechanical vibration of the CVD apparatus. Thus, the probability of making contact with a neighboring pillar should be high. The nearest-neighbor bridging of at least 80% can only be explained by a swing amplitude as large as the pillar spacing. Once a nanotube contacts a neighboring pillar, the growth orientation is fixed and the tube extends from one pillar to another.

Nanotubes can grow upward or downward from the pillar top. Downward-growing nanotubes just fall to the substrate. Upward-growing ones often form an arch between pillars. If the arch is long enough, its central part can touch the substrate surface due to vibration or rotation. This causes a nanotube to fall from both ends at the pillar tops, and explains the absence of tall arches. If two adjoining arches are formed, they can touch each other and become entangled (see Fig. 3(d) in Ref. 10).

6. Conclusion

We have succeeded in fabricating various types of suspended SWNT architectures on nano-scale pillar structures. These suspended SWNTs are either individuals or bundles, depending on the catalyst particle size and growth temperature. When the particle size is rather large, the SWNT yield is low and individual SWNT bridges are formed. For smaller catalyst particles, 5 nm or less, the SWNT yield increases, resulting in bundle formation. A higher yield is obtained for SiO_2 than for Si, as a result of the degree of silicidation of the catalyst particles. Thus, densely suspended bridges are formed between SiO_2 pillars. These suspended SWNTs show enhanced Raman and photoluminescence signals. Suspended SWNTs are formed in a self-assembling manner, probably due to vibration of the tips as the SWNTs grow. This growth characteristic is useful for site selective and directional synthesis of SWNTs. For future device applications, control of chirality is a crucial issue because the electrical and optical properties depend on the chirality of SWNTs.

7. Acknowledgments

References

[1] M. S. Dresselhaus, G. Dresselhaus, and Ph. Avouris (Eds.), "Carbon Nanotubes Synthesis, Structures, and Applications," Springer, Berlin, 2001.

[2] S. J. Tans, A. R. M. Verschueren, and C. Dekker, "Room-temperature Transistor Based on a Single Carbon Nanotube," Nature, Vol. 393, No. 7, pp. 49-51, 1998.

[3] S. J. Tans, M. H. Devoret, H. Dai, A. Thess, R. E. Smalley, L. J. Geerligs, and C. Dekker, "Individual Single-wall Carbon Nanotubes as Quantum Wires," Nature, Vol. 386, No. 3, pp. 474-477, 1997.

[4] K. Matsumoto, S. Kinoshita, Y. Gotoh, K. Kurachi, T. Kamimura, M. Maeda, K. Sakamoto, M. Kuwahara, N. Atoda, and Y. Awano, "Single-Electron Transistor with Ultra-high Coulomb Energy of 5000K Using Position Controlled Grown Carbon Nanotube as Channel," Jpn. J. Appl. Phys. Part. 1, Vol. 42, No. 4B, pp. 2415-2418, 2003.

[5] S. Frank, P. Poncharal, Z. L. Wang, and W. A. de Heer, "Carbon Nanotube Quantum Resistors," Science, Vol. 280, pp. 1744-1746, 1998.

[6] A. M. Cassell, N. R. Franklin, T. W. Tombler, E. M. Chan, J. Han, and H. Dai, "Directed Growth of Free-Standing Single-Walled Carbon Nanotubes," J. Am. Chem. Soc., Vol. 121, No. 34, pp. 1975-1976, 1999.

[7] N. R. Franklin and H. Dai, "An Enhanced CVD Approach to Exten-

sive Nanotube Networks with Directionality," Adv. Mater. Vol. 12, No. 12, pp. 890-894, 2000.

[8] Y. Homma, T. Yamashita, P. Finnie, M. Tomita, and T. Ogino, "Single-walled Carbon Nanotube Growth on Silicon Substrates Using Nanoparticle Catalysts," Jpn. J. Appl. Phys. Part 2, Vol. 41, No. 1, pp. L89-L91, 2002.

[9] Y. Homma, Y. Kobayashi, T. Ogino, D. Takagi, R. Ito, Y. J. Jung, and P. M. Ajayan, "Role of Transition Metal Catalysts in Single-walled Carbon Nanotube Growth in Chemical Vapor Deposition," J. Phys. Chem., Vol. 107, No. 44, pp. 12161-12164, 2003.

[10] Y. Homma, T. Yamashita, Y. Kobayashi, and T. Ogino, "Growth of Suspended Carbon Nanotube Networks on 100-nm-scale Silicon Pillars," Appl. Phys. Lett., Vol. 81, No. 12, pp. 2261-2268, 2002.

[11] Y. Jung, Y. Homma, T. Ogino, Y. Kobayashi, D. Takagi, B. Wei, R. Vajtai, and P. M. Ajayan, "High-Density, Large-Area Single-Walled Carbon Nanotube Networks on Nanoscale Patterned Substrates," J. Phys. Chem. B, Vol. 107, No. 28, pp. 6859-6864, 2003.

[12] Y. Kobayashi, Y. Homma, T. Ogino, Y. Ueno, O. Niwa, and T. Yamashita, "Extremely Intense Roman Signals from Single-walled Carbon Nanotubes Suspended between Si Nano-pillars," Chem. Phys. Lett., in press.

[13] M. J. O'Connell, S. M. Bachilo, C. B. Huffman, V. C. Moore, M. S. Strano, E. H. Haroz, K. L. Rialon, P. J. Boul, W. H. Noon, C. Kittrell, J. Ma, R. H. Hauge, R. B. Weisman, and R. E. Smalley, "Band Gap Fluorescence from Individual Single-walled Carbon Nanotubes," Science, Vol. 297, pp. 593-596, 2002.

[14] J. Lefebvre, Y. Homma and P. Finnie, "Bright Band Gap Photoluminescence from Unprocessed Single-walled Carbon Nanotubes," Phys. Rev. Lett., Vol. 90, No. 21, pp. 217401-1 - 217401-4, 2003.

[15] J. Lefebvre, J. M. Fraser, Y. Homma, and P. Finnie, "Photoluminescence from Single Walled Carbon Nanotubes: a Comparison between Suspended and Micelle-encapsulated Nanotubes," cond-mat/0308359; to appear in Appl. Phys. A (2004).

[16] Y. Zhang, A. Chang, J. Cao, Q. Wang, W. Kim, Y. Li, N. Morris, E. Yenilmez, J. Kong, and H. Dai, "Electric-field-directed Growth of Aligned Single-walled Carbon Nanotubes," Appl. Phys. Lett., Vol. 79, No. 19, pp. 3155-3157, 2001.

[17] A. Krishman, E. Dujardin, T. W. Ebbesen, P. N. Yianilos, and M. M. J. Treacy, "Young's Modulus of Single-walled Carbon Nanotubes," Phys. Rev. B, Vol. 58, No. 20, pp. 14013-14019, 1998.

[18] J-P. Salvetat, G. A. Briggs, J.-M. Bonard, R. R. Bacsa, A. J. Kulik, T. Stockli, N. A. Burnham, and L. Forro, "Elastic and Shear Moduli of Single-walled Carbon Nanotube Ropes," Phys. Rev. Lett., Vol. 82, No. 5, pp. 944-947, 1999.

Yoshikazu Homma
Group Leader, Device Physics Laboratory, NTT Basic Research Laboratories.

He received the B.S. and M.S. degrees in physics from Tohoku University, Sendai, Miyagi in 1976 and 1978, respectively. He received the Ph.D. degree in applied physics from the University of Tokyo, Tokyo in 1987. He joined the Musashino Electrical Communication Laboratories, Nippon Telegraph and Telephone Public Corporation (now NTT) in 1978. Since then he has engaged in research of ultra-trace analysis of semiconductors, *in situ* study of dynamic surface processes, and ordered nanostructure fabrication on semiconductor surfaces. His current interest is the growth control of carbon nanotubes and its *in situ* observation. He is a member of the Physical Society of Japan, the Japan Society of Applied Physics (JSAP), the Surface Science Society of Japan (SSSJ), the Japanese Society of Microscopy, and three other societies. He has received the Japanese Society of Microscopy award and several other awards.

Yoshihiro Kobayashi
Senior Research Scientist, Device Physics Laboratory, NTT Basic Research Laboratories.

He received the B.S., M.S., and Ph.D. degrees in chemistry and applied chemistry from Waseda University, Tokyo in 1983, 1985, and 1994 respectively. He joined the Musashino Electrical Communication Laboratories, NTT in 1985. Since then he has been researching reaction control on semiconductor surfaces and the fabrication of ordered nanomaterials. His current interest is the growth control of carbon nanotubes and its *in situ* observation. He is a member of the Physical Society of Japan, JSAP, and SSSJ.

Toshio Ogino
Professor, Dept. of Electrical and Computer Engineering, Yokohama National University, Hodogaya, Yokohama.

He received the B.E, M.E., and Ph.D. degrees in engineering from the University of Tokyo, Tokyo in 1974, 1976, and 1979, respectively. He joined the Musashino Electrical Communication Laboratories, Nippon Telegraph and Telephone Public Corporation (now NTT) in 1979. Since then he has researched semiconductor devices, surface processes, and ordered nanostructure fabrication on semiconductor surfaces. He moved to Yokohama National University in 2002. His current interest is the growth control of carbon nanotubes and its application to smart nano-interconnections. He is a member of JSAP, SSSJ, the Institute of Electronics, Information and Communication Engineers, and the Materials Research Society.